JOURNAL OF GEOPHYSICAL RESEARCH VOL. 69, NO. 1 JANUARY 1, 1964

High-Latitude Geophysical Studies with Satellite Injun 3

5. Very-Low-Frequency Electromagnetic Radiation

D. A. GURNETT[1] AND B. J. O'BRIEN[2]

Department of Physics and Astronomy
State University of Iowa, Iowa City

Abstract. This is a preliminary report of very-low-frequency (VLF) electromagnetic radiation measurements made by the Injun 3 satellite in the altitude range 250 to about 2000 km over North America from December 1962 to March 1963. The radiation is received by a loop antenna on the magnetically oriented satellite. Amplitude is measured with narrow-band filters at six frequencies, the lowest being 0.7 kc/s and the highest being 8.8 kc/s. A wide-band amplitude over the frequency band from 0.5 to 7.0 kc/s is also measured. In addition, the VLF signal modulates the telemetry transmitter so that a detailed spectral analysis can be made on the ground. It is found that the amplitude of naturally occurring VLF signals is commonly tens of decibels stronger at Injun 3 than on the ground, and this is to be understood as due to strong absorption of VLF energy in the ionosphere, as has been found previously in other experiments. The maximum observed signal strength over the band 0.5 to 7.0 kc/s is 5×10^{-2} gamma. The amplitude of VLF chorus, considered for local times between 0800 and 1300, shows a maximum at $L = 5$ over the three-day period studied. Simultaneous occurrences of VLF electromagnetic emission, auroral optical emissions, and particle precipitation into the atmosphere have been repeatedly observed. Two specific instances are discussed. In the more stable of the two, it is concluded that the auroral hiss was generated in the same magnetic shell in much the same region of the magnetosphere (near the outer boundary of trapping) as were the precipitated particles that caused the aurora. For this event it is estimated that, for the VLF radiation having frequencies less than 10 kc/s, the VLF energy flux at the satellite was about 8×10^{-7} erg cm^{-2} sec^{-1}, the energy flux of precipitated electrons was about 10 ergs cm^{-2} sec^{-1}, and that from the auroral light was about 0.6 erg cm^{-2} sec^{-1}. These measurements suggest that, in this event, the electrons caused both the visible aurora and the VLF hiss emission.

INTRODUCTION

Naturally occurring electromagnetic waves in the very-low-frequency (VLF) part of the spectrum have been the subject of many studies, particularly since the pioneering work of *Storey* [1953]. The frequency range of VLF is considered to extend from about 1 to about 30 kc/s [*Gallet and Helliwell,* 1959].

The origin of the VLF phenomenon called a 'whistler' is known to be a lightning discharge. The discharge causes an electromagnetic impulse called a sferic, which can be ducted about geomagnetic field lines to bounce from one hemisphere to another. As it travels through the dispersive ionized medium at high altitudes, different frequencies travel at different speeds, and instead of 'hearing' a click with an audio amplifier, one 'hears' a whistle. Whistlers have been used to study such features of the upper atmosphere and magnetosphere as the electron density [*Smith and Helliwell,* 1960; *Carpenter,* 1962].

However, many naturally occurring VLF signals other than sferics and whistlers can be received at ground-based observatories. Many of these signals have distinctive frequency-time (f-t) spectrums which are crudely reproducible. The various phenomena are classified on the basis of their f-t form and are called VLF emissions [see classification by *Gallet,* 1959]. The origin of many of these phenomena is unknown, and several of them may indeed have a common origin, so that the classifications are largely for experimental convenience. Since the origins are uncertain, most of the studies of

[1] Now Graduate Research Fellow of the National Aeronautics and Space Administration at the State University of Iowa.

[2] Now at the Department of Space Science, Rice University, Houston, Texas.

these phenomena have concentrated on describing when and where they occur, and with what other phenomena they occur, rather than on using them (as we do whistlers) to prove immediately and directly magnetospheric properties. The resultant organization of ground-based observations has been considerable [e.g., *Gallet*, 1959; *Helliwell*, 1962; *Martin*, 1960; and *Jones et al.*, 1963]. It is apparent that satellite measurements of these VLF signals could aid such organization (in principle, at least) by making rapid surveys of their latitudinal and longitudinal dependence, and so on.

But satellite observations of VLF phenomena have unique advantages over ground-based measurements, principally because the latter detect the VLF radiation after it has passed through and been attenuated by the ionosphere [*Leiphart*, 1962]. We summarize the disadvantages of ground-based observations compared with satellite observations as follows:

1. VLF waves propagating through the ionosphere are attenuated by approximately 35 db during the local day and approximately 10 db during the local night [*Leiphart*, 1962]. The magnitude of the attenuation is variable and relatively uncertain on any given occasion, so that we cannot accurately estimate the power originally in a given VLF signal from ground-based measurements.

2. VLF waves generated in the magnetosphere may enter the ionosphere and travel considerable distances in the earth-ionosphere wave guide before they reach a ground station [*Martin*, 1958]. It is therefore difficult to locate the source in the magnetosphere.

3. Man-made radiation (such as from harmonics of power systems) often interferes with ground-based observations, but the ionospheric attenuation of item (1) above minimizes the problem for satellite studies.

4. In simultaneous observations of VLF emissions and bombardment of the ionosphere by electrons (e.g., as in auroras), the very bombardment may increase ionospheric attenuation to the extent that the VLF emissions cannot be detected on the ground [*Morozumi*, 1962].

The disadvantages of making satellite observations rather than ground-based observations are the usual ones associated with satellite work, but, in our view, they do not outweigh the advantages.

The principal scientific aims of Injun 3 as they existed before launch were to measure auroral optical emissions, the precipitated particles causing them, and the VLF emissions that may interact with the precipitated and/or trapped electrons [*O'Brien et al.*, 1964]. This paper summarizes preliminary analysis of the VLF phenomena observed with Injun 3 at high latitudes and their association with other phenomena detected by the satellite. Specifically, we discuss the absolute amplitude of a VLF emission known as chorus as a function of the spatial position of the satellite for a selected period. Also, measurements and observations regarding the association between auroras, VLF electromagnetic emissions, and the precipitation of electrons into the atmosphere will be presented for several specific passes of the satellite over North America at times of geomagnetic disturbances.

We do not examine here the characteristics of whistlers observed by Injun 3, nor do we give a theoretical treatment of these results. Furthermore, the satellite is still operational at the time of writing (August 1963), and so this treatment is preliminary.

Experimental Details

A block diagram of the Injun 3 VLF experiment is shown in Figure 1. A loop antenna is used to detect the magnetic component of the electromagnetic wave in the frequency range of interest. The satellite is oriented by a large permanent magnet such that the geomagnetic field vector **B** is in the plane of the loop antenna. This orientation provides optimum coupling between the antenna and an electromagnetic wave propagating in the whistler (longitudinal extraordinary) mode [*Ratcliffe*, 1959]. In this mode of propagation the wave is characterized as essentially a circularly polarized wave propagating along the geomagnetic field line.

The VLF antenna and preamplifier have been designed in such a manner that the signal from the preamplifier is representative of the magnetic component of the electromagnetic wave coupling the loop antenna. (For a discussion of the instrument calibration, see the appendix.) The preamplifier signal is presented to a six-channel frequency spectrum analyzer from

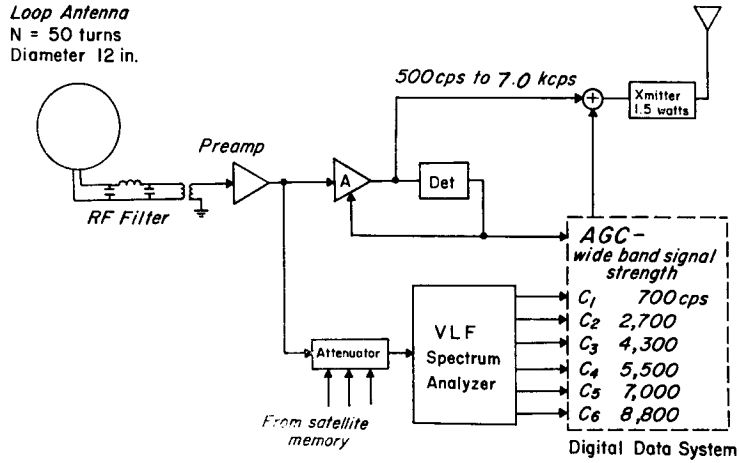

Fig. 1. Block diagram of Injun 3 VLF experiment.

which the absolute amplitude of the magnetic component of the wave can be determined at six frequencies: 0.7, 2.7, 4.3, 5.5, 7.0, and 8.8 kc/s, respectively. Each frequency channel samples a 50-cps band of the frequency spectrum. The frequency response of a typical spectrum analyzer channel is shown in Figure 2. The dynamic range of the spectrum analyzer is 40 db. The dynamic range can be shifted in two 20-db steps with an attenuator controlled by the satellite memory. Analog to digital converters in the satellite data system quantize the 40-db dynamic range into sixteen steps, each step 2.5 db wide. The output from a specific channel is processed by the satellite data system in such a way that the satellite transmits the *minimum* amplitude occurring in the time interval since the previous sample was transmitted. The rate at which a given analyzer channel may be sampled is controlled by the satellite memory. The maximum sampling rate is 12 samples/sec. The sampling mode most commonly used in orbit is 1 sample every 2 sec. Because the minimum amplitude occurring over an interval of time is sampled, the spectrum analyzer measurement gives the absolute amplitude distribution of the slowly varying background noise spectrum and ignores the transient noise burst whose time constants are much shorter (less than 0.1 sec) than the sample interval. The spectrum analyzer measurement does not, therefore, respond to lightning impulses.

The preamplifier signal, limited to a frequency band of approximately 0.5 to 7.0 kc/s and normalized to a constant amplitude by an automatic gain control (AGC) circuit, is used to directly modulate the telemetry transmission at 136.860 Mc/s. The VLF signals thus telemetered to the ground can be analyzed with high time resolution spectrum analysis equipment. The automatic gain control feedback voltage is used as a measure of the rms wide-band magnetic field strength in the frequency band 0.5 to 7.0 kc/s. The frequency response of the wide-band VLF system, with the gain of the AGC circuit held constant, is shown in Figure 3. The response time constant of the automatic gain control feedback loop is approximately 0.2 sec.

The Injun 3 VLF experiment, therefore, provides three measurements: (*a*) the absolute

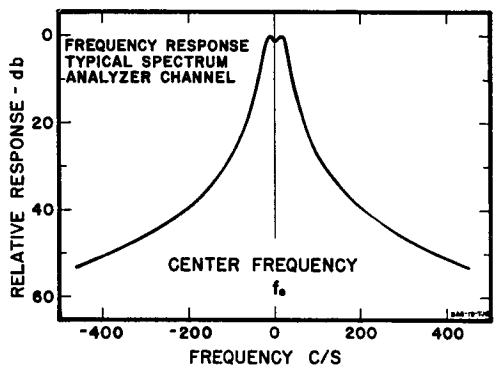

Fig. 2. Frequency response of a typical spectrum analyzer channel.

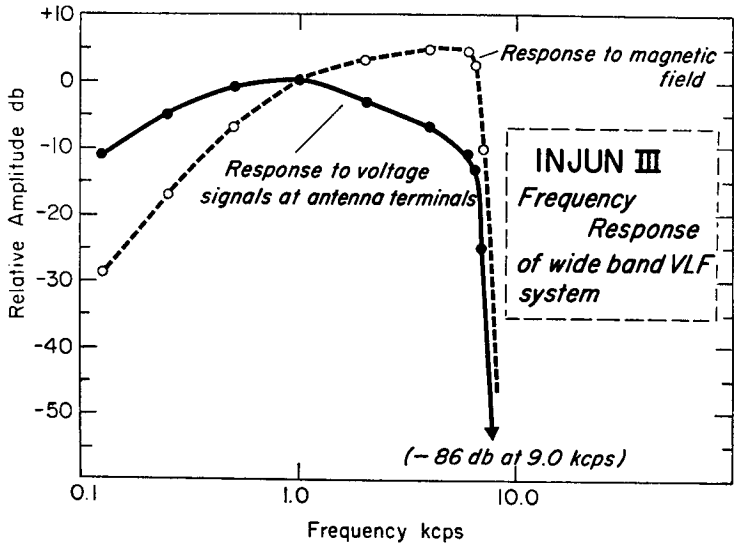

Fig. 3. Frequency response of the wide-band VLF system.

spectral density of the VLF radiation at six frequencies, 0.7, 2.7, 4.3, 5.5, 7.0, and 8.8 kc/s; (*b*) the wide-band signal strength between 0.5 and 7.0 kc/s; and (*c*) high resolution frequency-time spectrums from the wide-band VLF signal which is telemetered to the ground.

These measurements are complementary to one another. For example, high time resolution frequency-time spectrums cannot be obtained from the satellite-borne spectrum analyzer because of its low sampling rate. The wide-band VLF signal telemetered to the ground may, however, be processed with high time resolution analyzers such as the Rayspan spectrum analyzer. VLF spectral characteristics resembling time-stationary white noise may be indistinguishable from communication noise to an observer who uses the wide-band VLF signal telemetered to the ground. Slowly varying spectrums of this type are, however, analyzed easily by the satellite-borne spectrum analyzer.

Many of the ground-based studies of VLF phenomena concentrate on the frequency-time characteristics of the emissions rather than on their amplitude. This is because the amplitude measured on the ground is so modified by considerations listed in the introduction. We wished to make amplitude measurements to compare them with magnitudes of particle fluxes and auroral light. The lower limit to our amplitude measurements was set, as usual, by receiver noise.

The noise level of the receiver stated in terms of an equivalent magnetic spectral density applied to the antenna is approximately 5.0×10^{-11} (gamma)^2 (c/s)$^{-1}$ (see the appendix). Treating the lower atmosphere as a nonconducting medium with an index of refraction of unity, this equivalent receiver noise level corresponds to a VLF spectral power density of approximately 1.5×10^{-14} watt (m)$^{-2}$ (c/s)$^{-1}$. Ellis says that VLF flux densities from magnetosphere VLF emissions observed by him, on the ground, range from 6×10^{-19} to 10^{-16} watt (m)$^{-2}$ (c/s)$^{-1}$ [*Ellis*, 1959]. It appears, therefore, that the sensitivity of the Injun 3 VLF receiver is not, in general, adequate at ground level for detecting magnetospheric VLF emissions.

However, it was anticipated before launch that the following factors would operate to increase the intensity of the magnetic component of a VLF wave (of magnetospheric origin) at the satellite relative to a ground-based observation. First, in a plasma, for a given wave power, more of the energy is stored in the magnetic component. Second, a VLF electromagnetic wave generated in the magnetosphere and reaching the satellite will not be attenuated by the ionosphere. Third, if VLF electromagnetic waves are radiated essentially isotropically from

the source region, very large VLF power fluxes may be observed when the satellite is close to the source. Fourth, if magnetospheric ducting of VLF waves occurs, the VLF power density in the duct at large distances from the source may be comparable to the power density in the source region. Thus, a very intense VLF power flux may be observed when the satellite is in a duct [*Smith et al.*, 1960].

At the time that the Injun 3 experiment was designed, the only direct observations of naturally occurring VLF signals above the ionosphere came from whistler observations with Vanguard 3 [*Cain et al.*, 1961]. Estimates of whistler amplitudes obtained from these observations indicated that the magnetic component of whistlers propagating in the magnetosphere occasionally exceeds one gamma (10^{-5} gauss). This amplitude is relatively large compared to ground-based observations and encouraged the view that the Injun 3 VLF experiment had sufficient sensitivity to make meaningful measurements in the magnetosphere. In fact, as will be seen, the actual sensitivity is quite adequate in flight, and signals above the threshold of sensitivity are commonly observed in high-latitude passes of Injun 3 over North America.

Satellite-borne instruments that have preceded Injun 3 in making measurements and observations of VLF radiation in the magnetosphere have been included on the Vanguard 3 [*Cain et al.*, 1961], Lofti 1 [*Leiphart*, 1962], and Alouette [*Barrington and Belrose*, 1963] satellites.

Observation of VLF Phenomena with Injun 3

VLF electromagnetic phenomena are classified by the manner in which the spectral character of the emission changes with time, as displayed on a frequency-time spectrogram. *Gallet* [1959] lists the following classifications:

1. Whistlers whose source is lightning.
2. VLF emissions not associated with lightning, either (*a*) continuous or (*b*) discrete.
3. Interactions between whistlers and VLF emissions.

Whistlers are VLF electromagnetic impulses generated by lightning that have had their frequency-time spectrums modified as the result of dispersive propagation over very long paths through the magnetosphere [*Helliwell and Morgan*, 1959]. We show in Figure 4 an example of a frequency-time spectrogram of a whistler observed with Injun 3. The darkened part of the spectrogram indicates the more intense signal. Whistlers will not be analyzed here; they have been observed by other satellites [*Cain et al.*, 1961; *Barrington and Belrose*, 1963].

The spectral classification of VLF emissions in the Injun 3 studies is made from frequency-time (*f-t*) spectrograms of the wide-band VLF signal telemetered to the ground. We generate *f-t* spectrograms in two ways. The two analyzers differ in that the first, the comb-filter high resolution analyzer, provides time resolution of approximately 10 msec. For the second type, the sweep-filter analyzer, the time resolution is approximately 2 sec. Spectrograms are usually presented on photographic film or some type of photosensitized paper. Examples of wide-band VLF signals telemetered from the satellite to the ground and analyzed with low and high resolution analyzers are shown in Figure 5 and Figure 6, respectively. The dark part of a spectrogram indicates the stronger signal. Corresponding points on the low and high resolution spectrograms can be found at $L = 4$, 1453 UT, on the December 19 data. The analyzers used for low and high time resolution spectrograms in this analysis are, respectively, the Proboscope Model SS-100 and the Raytheon Rayspan analyzer. Many of the commonly occurring VLF emissions can be identified with low resolution spectrograms.

Our nomenclature for the various classes of VLF phenomena will follow as closely as possible the presently accepted terminology [*Gallet*, 1959]. Two classes of VLF phenomena selected for study here are 'chorus' and 'auroral hiss.'

The presence of a *chorus emission* can be identified from the Injun 3 VLF measurements

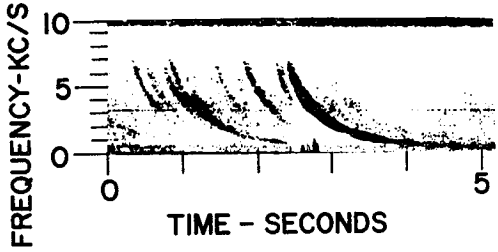

Fig. 4. Frequency-time spectrogram of a whistler.

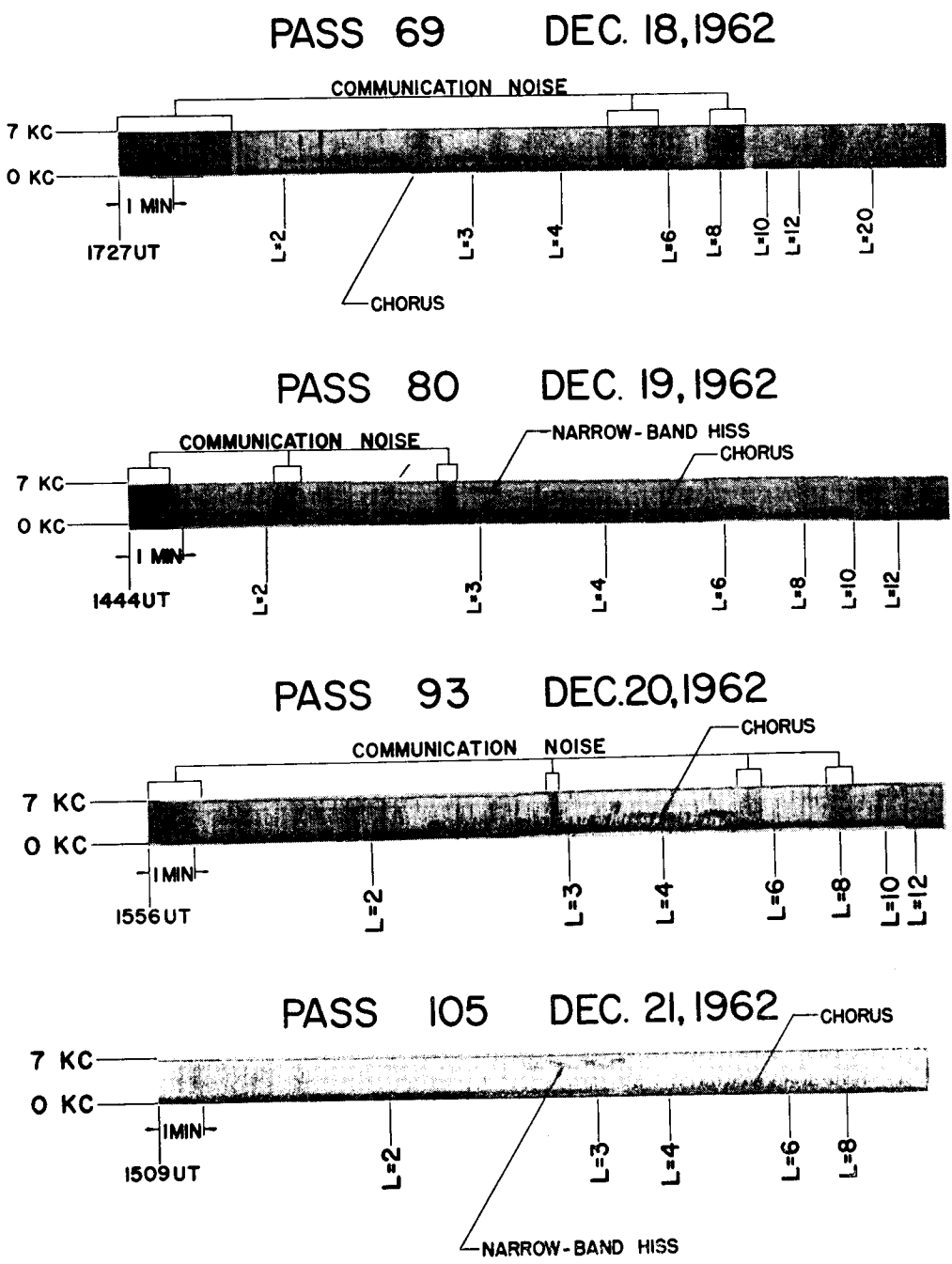

Fig. 5. Low time resolution spectrograms of chorus.

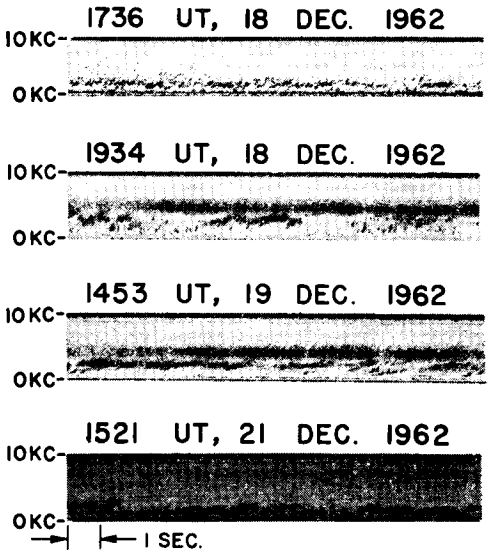

Fig. 6. High time resolution spectrograms of chorus at $L = 4$.

in the wide-band VLF signal telemetered to the ground. The spectral character associated with a chorus emission can usually be identified with high time resolution spectrograms, low time resolution spectrograms, or aural monitoring. Also, the distinct rising tones characteristic of chorus emission tend to start and terminate abruptly. When a chorus emission is being detected by the satellite VLF receiver, considerable fluctuations usually exist in the wide-band signal strength measurement. Low time resolution spectrograms usually show chorus as irregular blotches extending over the emission bandwidth (see Figure 5). If the low resolution spectrogram shows a spectrum characteristic of chorus and the wide-band signal strength is fluctuating rapidly, it is considered that there is a good indication of a chorus emission. Positive identification is always made by aural monitoring or high time resolution spectrograms.

The presence of an *auroral hiss emission* can be identified best from the Injun 3 VLF measurements by using the satellite-borne spectrum analyzer data. The magnetic spectral density of the VLF hiss radiation at the satellite is measured for each of the six analyzer frequencies. An auroral hiss emission is a wide-band noise signal and appears as a simultaneous response from all the VLF spectrum analyzer channels above approximately 4 kc/s. The wide-band signal strength measurement can be used to complement the spectrum analyzer measurements. Wide-band hiss cannot always be positively identified using only the wide-band VLF signal telemetered to the ground because the VLF signal may not be distinguishable from communication noise.

We shall now consider the possible satellite coordinates in space and time and their significance relative to an observation of a VLF electromagnetic wave at the satellite.

Inferences regarding the nature and spatial distribution of the VLF source from measurements at the satellite require knowledge of the viewing region of the VLF antenna into the ionosphere and magnetosphere, i.e., of the propagation conditions from the source to the satellite as well as the directional properties of the antenna. The nature of this viewing region has to our knowledge never been subjected to experimental, quantitative measurements using a magnetospheric VLF source, although relevant theoretical treatment of VLF propagation has been given, for example, by *Storey* [1953], *Hines* [1957], and *Smith* [1961]. It appears that VLF electromagnetic energy is guided along geomagnetic field lines by field-aligned ionization in the magnetosphere [*Smith*, 1961].

For purposes of qualitative discussion in this note, a very general model has been hypothesized to aid in the interpretation of the Injun 3 VLF data. The model illustrated in Figure 7 has been constructed assuming that there exists some surface having symmetry about a geomagnetic field line within which VLF electromagnetic waves can propagate to the satellite. Outside this surface, propagation of VLF waves to the satellite is inhibited. Three regions of propagation are defined in this model. In region

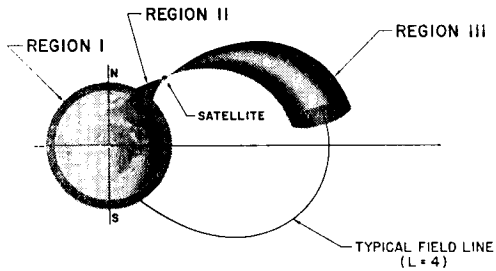

Fig. 7. Viewing region of the VLF antenna.

I, VLF waves propagate in the earth-ionosphere wave guide. Lightning is considered the only significant source of VLF radiation occurring in region I. Region II is between the satellite and lower boundary of the ionosphere. VLF electromagnetic waves in region II propagate to the satellite in the whistler (longitudinal extraordinary) mode. Lightning impulses generated in region I and coupled into region II are attenuated in traversing the ionosphere. Region III is considered to extend outward into the magnetosphere above the satellite as illustrated in Figure 7. It will be seen that we do not determine here whether VLF chorus detected by Injun 3 arises in region II or III, although the VLF hiss studies given here were made at such low altitudes (250 km to 300 km) that region II probably shrank to negligible dimensions.

The validity of the model presented here rests largely on the extent to which heavy ions allow propagation to occur at large angles to the geomagnetic field lines. For a discussion of the effects of heavy ions on the propagation of a VLF electromagnetic wave, see, for example, *Hines* [1957].

One of the unique features of satellite observations is the ability to carry out rapidly extensive latitude surveys of a given phenomenon. Further, with Injun 3 we measure simultaneously Van Allen radiation and other phenomena (see part 1 for a complete description of the satellite). For such studies it proves useful to replace the three geographic coordinates of longitude, latitude, and altitude with two magnetic coordinates L and B [*McIlwain*, 1961]. The parameter L specifies a magnetic shell on which a trapped particle bounces in latitude and drifts in longitude. It similarly can roughly specify a line of force in the geomagnetic field that is not only a 'guiding center' for a trapped or precipitated particle but also a guiding center of a bouncing or propagating VLF signal. The unit of L is an earth radius (6370 km). Numerically, L is such that in a perfect dipole field it would be the equatorial radial distance to the magnetic shell. The unit of B, the magnetic field strength, is the gauss.

Because the electron density and hence the index of refraction is strongly altitude dependent, the geocentric distance or satellite altitude must be considered a relevant coordinate in the analysis. Ground-based VLF observations have established a variation in the occurrence rates of various VLF phenomena with local time [*Allcock*, 1957]. The VLF observations performed with Injun 3 may, therefore, be considered as functions of the L shell parameter, B, the altitude of the satellite, and the local time at the satellite.

Experimental Results

Detectable VLF phenomena. We shall agree to recognize the presence of a VLF signal at the satellite, when either (1) the quantized decimal readout of the wide-band signal strength (AGC) measurement is greater than 3 (corresponding to 10^{-3} gamma, see appendix) or (2) when a VLF spectrum characteristic of the phenomena can be recognized from the wide-band VLF signal telemetered to the ground. The threshold for recognition of a VLF phenomenon using the telemetered wide-band VLF signal is highly dependent on the spectral character of the phenomenon and is always less than 10^{-3} gamma when the communication signal to noise ratio exceeds 20 db, as it does when useful digital data are accepted by the computer that does the data reduction. VLF phenomena of a discrete transient nature may be recognized with the telemetered wide-band signal but may not give a detectable AGC measurement because of the slow sampling rate for this measurement (1 sample every 4 sec). It is possible, therefore, that a strong whistler may be recognized aurally with the telemetered wide-band VLF signal, but the AGC may not be sampled at the proper instant to determine the amplitude of the whistler.

Noise impulses showing little dispersion are commonly observed at the satellite via the wide-band VLF signal telemetered to the ground. These impulses are presumed to be sferics, which have propagated a relatively short distance from region I, through region II, and to the satellite. Barrington calls noise impulses of this type, observed in the ionosphere, short fractional-hop whistlers [*Barrington and Belrose*, 1963]. Long fractional-hop whistlers are sferic impulses that have crossed the magnetic equator in propagating through the magnetosphere. Long fractional-hop whistlers are also commonly observed at the satellite.

No quantitative studies have been attempted concerning the propagation of whistlers in the

magnetosphere. Some qualitative statements are, however, in order. Sferic impulses could always be heard during tests on the ground using the satellite VLF receiver and antenna. However, for the total observation time on the ground, estimated to be 15 hours extending over two months, only three whistlers and no VLF emissions of any type were identified. After the satellite was launched, the same receiver and antenna have detected many long fractional-hop whistlers in the ionosphere. In some instances as many as 20 long-hop whistlers per minute have been heard. It has also been observed that the background sferic (short fractional-hop whistlers) noise level in the ionosphere is much lower than on the ground. Instances have been found where no VLF sferic impulses were detectable at the satellite for more than 25 minutes. A steady background of sferic impulses could always be heard with the satellite receiver and antenna on the ground. These observations serve to illustrate the large ionospheric attenuation occurring when VLF electromagnetic waves propagate from region I to region II (see the viewing region model, Figure 7).

A relatively rare phenomenon, which has been observed with the Injun 3 VLF receiver on several occasions, is the excitation of VLF emissions by sferic impulses that have propagated to the satellite. The emissions, which always start immediately after the triggering whistler, are often of an exceedingly complex frequency-time structure consisting of several tones of changing frequency. Enhancement of whistler-triggered emissions appears to occur during certain times. Passes have been observed in which 40 per cent of all sferic impulses observed at the satellite were followed by emissions, even for relatively weak impulses. Other passes occur in which no triggered emissions occur, even when very strong sferic impulses are observed. No detailed quantitative studies are attempted here of the propagation of sferic impulses in the magnetosphere medium.

The rest of this paper will consider only VLF phenomena of the class known as VLF emissions [*Gallet*, 1959]. Of all the observations telemetered by the satellite during January 1963, VLF electromagnetic waves, associated with VLF emission phenomena, were present at the satellite with sufficient intensity to exceed the detectability threshold of the wide-band signal strength measurement for 24 per cent of the total received telemetering time. Satellite data received at high geomagnetic latitude stations such as College, Alaska, show measurable VLF emissions for as much as 60 per cent of the observation time during January.

The maximum rms amplitude VLF radiation observed with the wide-band signal strength measurement during January 1963 was 5×10^{-3} gamma. This observation was made at 1554 UT, January 30, 1963. The L coordinate of the satellite was $L = 6$, and the satellite altitude was 320 km. In this instance the VLF phenomenon was a wide-band hiss emission of the type usually associated with auroras. The magnetic spectral density of the hiss radiation for this instance, calculated on the basis of a 7.0-kc/s receiver bandwidth, is 3.6×10^{-7} $(\text{gamma})^2$ $(\text{c/s})^{-1}$. Ellis gives 10^{-16} watt $(\text{m})^{-2}$ $(\text{c/s})^{-1}$ as the maximum spectral power density of auroral hiss observed by him on the ground [*Ellis*, 1959]. This spectral power density corresponds to a magnetic spectral density of 4.3×10^{-18} $(\text{gamma})^2$ $(\text{c/s})^{-1}$. The maximum magnetic spectral density of auroral hiss observed by Injun 3 in the ionosphere, therefore, exceeds the maximum magnetic spectral density of auroral hiss observed on the ground (as observed by Ellis during previous studies) by a factor of 10^6. These observations serve to illustrate the intensity of VLF electromagnetic radiation observed with Injun 3.

Hiss having frequencies less than 1 kc/s and chorus are the electromagnetic emissions most commonly observed at the satellite. Hiss in this frequency range will be called extra-low-frequency (ELF) hiss. In many cases ELF hiss observed at the satellite having frequency components as low as 200 cps can be recognized with frequency-time spectrograms obtained from the wide-band VLF signal telemetered to the ground. At 200 cps it is seen from Figure 3 that the frequency response of the wide-band VLF receiver is down 22 db from the midband value. The ELF hiss is often characterized by a sharply defined upper frequency limit. The absolute spectral densities of frequencies less than 1 kc/s are difficult to analyze because of the nonuniform frequency response of the VLF receiver-antenna system at these frequencies. No comprehensive quantitative study has been attempted of ELF hiss emissions observed at the

satellite. Because man-made radiation makes ground-based observations at ELF frequencies difficult, the rather common observations of electromagnetic emissions in the ELF region with Injun 3 are considered of potential importance in the study of magnetospheric phenomena.

VLF chorus emissions observed with Injun 3. We shall now investigate the nature and amplitude of the VLF electromagnetic radiation from chorus emissions as a function of the spatial coordinates of the satellite. As discussed earlier, an appropriate set of satellite coordinates for the investigation of VLF phenomena would be the local time at the satellite, the altitude of the satellite, and the L shell parameter associated with the geomagnetic field line passing through the satellite. The periodic nature of the satellite trajectories through these coordinates allows the repeated observation of VLF activity in a selected region of this coordinate space. A general observation from Injun 3 has been that chorus emissions are observed consistently from pass to pass over some limited part of the orbit. Because numerous other magnetospheric phenomena are strongly dependent on the L shell parameter, it was decided that the amplitude of VLF chorus radiation at the satellite would be investigated as a function of this parameter. To conveniently study the L dependence of the amplitude of chorus radiation, it would be desirable to hold the local time and altitude coordinates constant while varying L. As the local time and altitude coordinates cannot be held constant because of the orbit, data must be selected that minimize the variations in these coordinates, or it must be demonstrated that the amplitude of chorus radiation is not a significant function of these coordinates for the ranges investigated.

Variations with local time can be minimized by selecting only passes for which the L coordinate increases or decreases very rapidly with local time. A series of satellite trajectories in L and local time coordinates is shown in Figure 8. Using the criterion that acceptable passes cover the range of L values from 2 to 10 for local times between 0800 and 1300, we selected six passes for analysis. The revolution numbers associated with these passes are 69, 70, 71, 80, 93, and 105. The average planetary geomagnetic K_p index for the three-day period being considered was approximately 5. During this period the satellite was not aligned with the geomag-

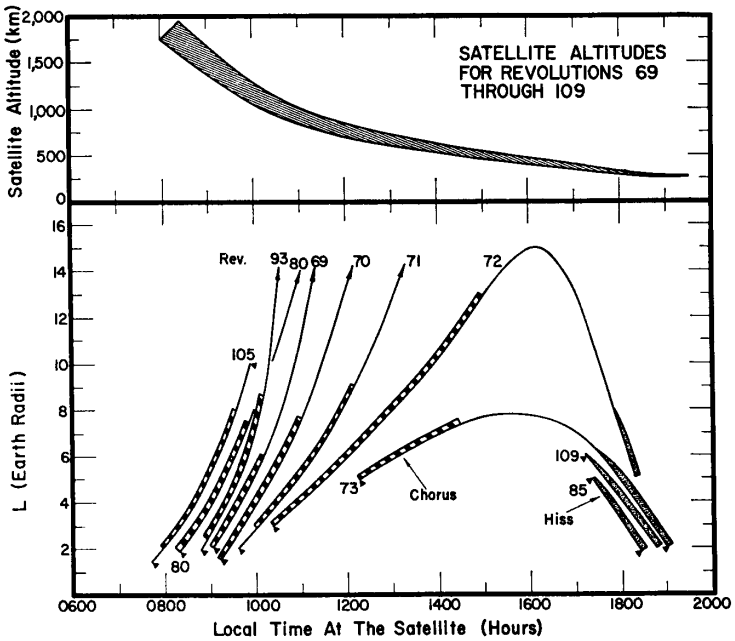

Fig. 8. Chorus and hiss observations in L and local time coordinates.

netic B field because oscillations associated with the injection into orbit had not yet damped. Because we do not have prior knowledge of the ray directions associated with VLF radiation from chorus emissions, we will not attempt to correct for the variable antenna orientation. The magnetic aspect sensors on the satellite showed that the orientation of the loop antenna relative to the geomagnetic field did not have the same dependence on L from pass to pass.

Low resolution spectrograms typical of the VLF emissions observed at the satellite during these passes are shown in Figure 5. Using high resolution spectrograms, we established that the most intense VLF emission occurring during each of the selected passes was chorus. Chorus appears on the low resolution spectrograms as irregular blotches from 1 to 4 kc/s and predominantly for L values between 2 and 6. The extent to which VLF chorus emissions were detectable with the wide-band VLF signal strength measurement and identifiable with high resolution spectrograms is shown symbolically in Figure 8. Since chorus was the most intense VLF emission occurring during the selected passes, the wide-band VLF magnetic field strength measurement can be taken as a measure of the rms amplitude of the magnetic component of the VLF chorus radiation coupling the loop antenna.

The result of an analysis of the dependence of the wide-band signal strength measurement on the L shell coordinate of the satellite for the selected passes is shown in Figure 9. For each pass an average rms wide-band magnetic field strength (in gammas) was determined for each integral L value by calculating the average value of the wide-band magnetic field strength measurements between $L - 1/2$ and $L + 1/2$. The altitude and local time coordinates of the satellite were calculated for each integral value of L. The following items have been tabulated for each integral value of L and for each of the selected passes: (a) the rms wide-band magnetic field strength measurements averaged from $L - 1/2$ to $L + 1/2$; (b) the altitude of the satellite; and (c) the local time coordinate of the satellite. The six selected passes provide approximately 1200 data points distributed over L values from 2 to 14. The results shown in Figure 9 were obtained by averaging item (a) over the six selected passes for each integral value of L. The standard deviation of this average is shown as σ. The dependence of the average rms wide-band signal strength, tabulated as item (a), on the satellite altitude and local time coordinates are shown as scatter diagrams in Figure 10 and Figure 11, respectively. For the six selected passes, the spatial dependence of the amplitude of VLF chorus radiation observed at the satellite is, therefore, presented collectively by the result shown in Figures 9, 10, and 11.

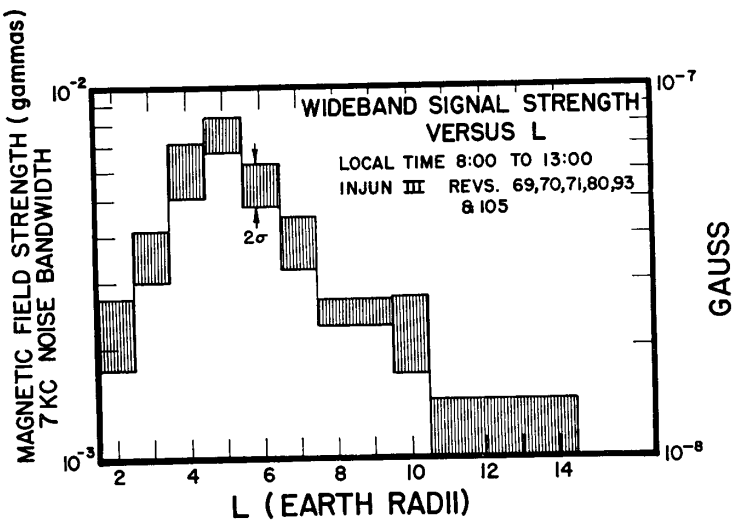

Fig. 9. The amplitude of VLF chorus radiation versus the satellite L coordinate.

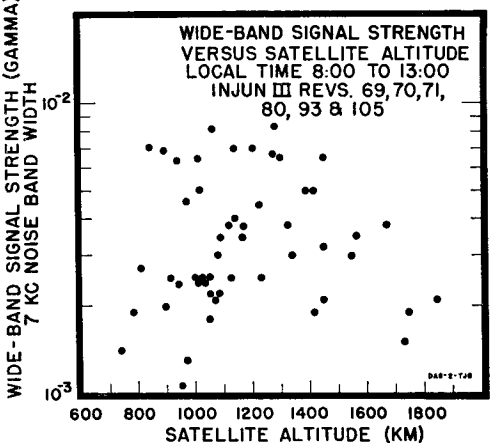

Fig. 10. The amplitude of VLF chorus radiation versus satellite altitude.

The results just presented will be used to support the following hypothesis. Of the three coordinates considered and their respective ranges, the amplitude of VLF chorus radiation observed at the satellite for the six selected passes depends primarily on the L shell coordinate of the satellite and is as shown in Figure 9. The scatter diagrams of Figures 10 and 11 show that any dependence on the other two variable parameters, altitude and local time, is insignificant in these samples for the ranges considered.

The amplitude of the VLF chorus shows an L dependence having a well-defined maximum at $L = 5$. The relatively small standard deviation of the measurements indicates that the amplitude of the VLF chorus radiation in successive passes was highly reproducible at each L value during the three-day period studied. The L parameter, as well as being a position coordinated for the satellite, was considered earlier to define the region of the magnetosphere viewed by the VLF antenna. If the model viewing region of the VLF antenna, as hypothesized in Figure 7, is accepted, the observed dependence of the amplitude of chorus radiation on L strongly suggests that the source of the discrete VLF chorus emissions is most intense somewhere in the vicinity of the $L = 5$ geomagnetic shell. This shell intersects the ground in North America at a magnetic latitude around 63°. These observations are for a specific three-day period and do not represent a general result applicable to all chorus emissions.

The spectral character of VLF chorus emissions has been compared at specific values of L for each of the selected passes. High time resolution spectrograms of VLF chorus emissions observed at the satellite for $L = 4$ are shown in Figure 6 for four of the six selected passes. The universal time for each of these observations is noted. We shall consider the maximum and minimum frequency occurring in the emission spectrums as characterizing the chorus emission. It can be seen from Figure 6 that the spectral character of the VLF chorus emissions is not necessarily the same for observations in the same region of space (same L values, local time differing by less than 2.5 hours, and satellite altitudes differing by less than 400 km) at times differing by one revolution period, or about two hours. It appears, therefore, that the spectral nature of VLF radiation from chorus emission observed at the same region in space can change markedly in times less than two hours.

Using high resolution spectrograms of VLF chorus emissions detected with Injun 3, we can find instances of the chorus emission occurring over a narrow band of frequencies. This banded type of chorus emission can be characterized by a fairly well-defined center frequency. In several instances it has been observed that the center frequency of the emission is remarkably independent of L, as though the VLF radiation

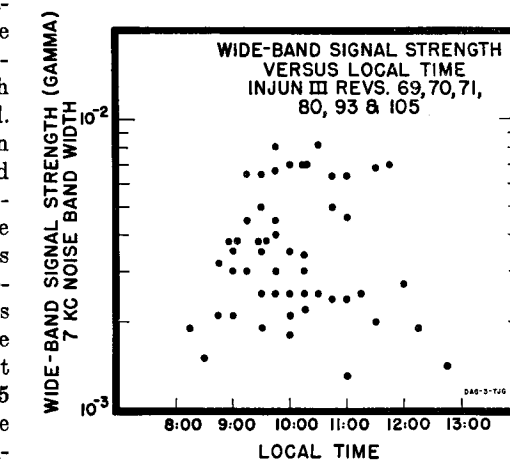

Fig. 11. The amplitude of VLF chorus radiation versus local time at the satellite.

from the same source region were being detected over a range of L values.

Auroral hiss emissions observed with Injun 3. We shall now present two observations obtained from Injun 3 which illustrate the simultaneous occurrence of VLF hiss, auroral optical emissions, and particle precipitation into the atmosphere. In these observations, which were an ultimate aim of the scientific design of the integrated payload (see part 1), many of the other instruments on the satellite were used, and we will describe their use very briefly here (see part 1 for a more complete description).

We examined passes over North America which took place after the injection spin and tumble damped out, when the satellite axis became oriented parallel to the local magnetic field vector **B** to within about 4°. The period studied was for times when both the satellite and the ground were in the dark and when the moon did not illuminate the ground so that the auroral photometers could be used. The photometers view the ground near the base of the geomagnetic field line passing through the satellite. They therefore detect auroras caused by precipitated particles which may be observed with other detectors (such as a Geiger tube detector 5, see part 1) on the satellite.

During many such passes in January through March 1963 the photometers detected auroras over North America in the auroral zone around $L \sim 6$ to 10. A report of these auroral studies per se is given by *O'Brien and Taylor* [1964] in part 4. We chose examples of bright auroras, then examined photometric, particle, and VLF data, and present examples of their interrelationship here. Because the features in these passes are so complex and variable, the examples presented here should not be regarded as 'typical.' However, they were selected simply on the basis of the brightness of the auroral light without regard to either VLF or particle characteristics. They therefore do represent an unbiased sample of the interrelationships of the three phenomena. Several dozen suitable passes are available, but only two are discussed in detail here. The variation of several parameters in these passes is presented in Figures 12 and 13. The satellite altitude in these passes ranged between 250 and 350 km.

Some general considerations applicable to both Figures 12 and 13 will now be presented, and then a detailed analysis of each will be made separately.

Besides the VLF experiment, there are twenty-one other detectors on Injun 3. Most of these provide information relevant to this study, but it is clearly impractical to present all data here. We therefore selected (*a*) for the VLF experiment, the wide-band (AGC) signal and the signals in three narrow-band channels at 2.7, 5.5, and 8.8 kc/s; (*b*) for auroral light, the 3914 A photometer; and (*c*) for particle flux, the counting rate of detector 5. Relations of these selected detectors with others on Injun 3 are discussed in the accompanying papers. Analysis of the spectrums of electrons and the absence of protons are discussed in part 2. Analyis of the angular distributions and dynamics of particle precipitation are discussed in part 3. Analysis of auroral studies is presented in part

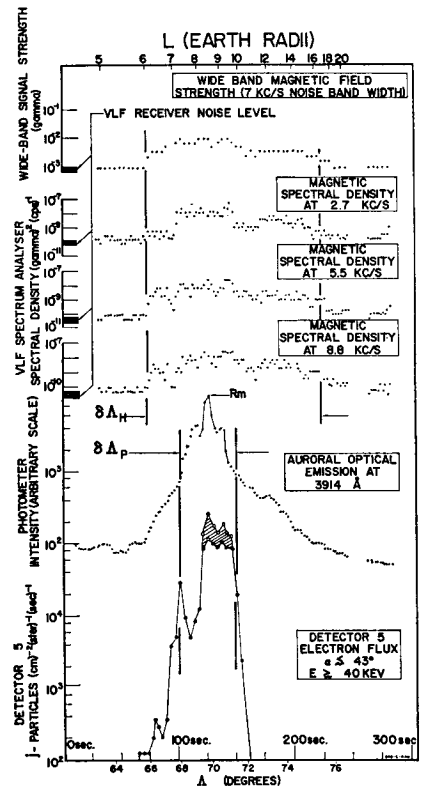

A SIMULTANEOUS OBSERVATION OF VLF ELECTROMAGNETIC EMISSION, AURORAL OPTICAL EMISSION, AND PRECIPITATED ELECTRONS 0720 TO 0725 UT

Fig. 12. The March 3, 1963, observation.

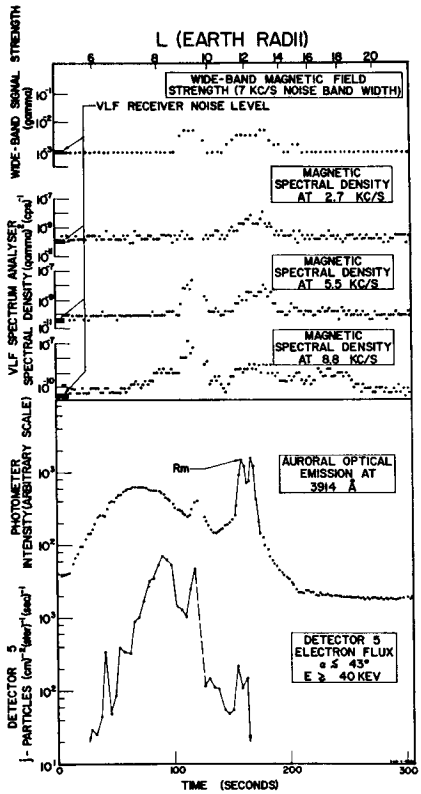

Fig. 13. The February 28, 1963, observation.

4. We therefore assume a familiarity with these earlier papers, and do not justify in detail our analysis of data from detectors other than the VLF. Similarly, the accuracy limitations of the measured brightness of the auroral light and so on are not discussed in this paper.

The sampling rates of the instruments in these passes were as follows: 1 sample every 0.25 sec for detector 5; 1 sample every 2.0 sec for the photometer and for the narrow-band VLF measurements; and 1 every 4.0 sec for the wide-band (AGC) signal. For the photometer and detector 5 the telemetered information gives an average over the sample interval. For the narrow-band VLF it gives a minimum over the sampling interval, and for the AGC it gives an instantaneous (~0.1-sec-duration) measure at the sampling instant. Therefore some care must be taken in quantitative use of these data. The points plotted for detector 5 are actually 4-sec averages of sixteen measurements, so as to use a time scale similar to that of the other instruments.

Analysis of the Observation of March 3, 1963

A simultaneous enhancement of the intensity of VLF electromagnetic radiation, auroral optical emission, and precipitated electrons is evident in the observation of March 3 shown in Figure 12. An aircraft was flying parallel to the satellite trajectory and making auroral observations at the same time (J. Evans and M. Walt, private communication) but no detailed analysis of the aurora is presented here.

The VLF spectrum analyzer shows that the magnetic spectrum is essentially a flat noise spectrum starting below 2.7 kc/s and extending above 8.8 kc/s. The response of the 4.3- and the 5.5-kc/s channels was similar in character and amplitude to that of the three channels plotted. It is apparent from Figure 12 that there is good general agreement between an estimate of the VLF magnetic spectral density integrated over each narrow channel and the AGC wide-band signal strength measurements when account is taken of the different techniques of sampling (discussed above).

We identify the VLF emission occurring in this event as an auroral hiss emission on the basis of the characteristic wide-band noise spectrum and the close association between the VLF hiss and the auroral optical emissions. We will now discuss the association between the VLF emission, the auroral optical emission, and the precipitated electrons as seen in the temporal frame of reference of the satellite during the March 3 event. Reference will be made to the L shell parameter as a coordinate. It must be remembered, however, that it is not possible to separate temporal and spatial dependences in this observation. Note that all the data are plotted in Figure 12 on logarithmic scales and that the signals in the VLF and the photometer rise from a level which is essentially the noise level of the detectors. Thus it is not possible to compare quantitatively the *initial* increases in the signals seen by the several detectors.

It is apparent, however, that at $L = 6$ (or invariant latitude $\Lambda \sim 66°$) the VLF emission, the auroral light, and the flux of *precipitated*

electrons began to increase rapidly in magnitude. The flux of *trapped* electrons (with $E_e \gtrsim 40$ kev) at this point and for about one minute beforehand was about (3×10^4) particles cm^{-2} sec^{-1} $ster^{-1}$. The flux of trapped particles started to increase appreciably above this level when the flux of precipitated electrons became comparable with it, and essentially the behavior of trapped and precipitated electrons is such as to approach isotropy over the upper hemisphere, as usual in such events (see part 3).

As we view the data plotted in Figure 12, it is seen that the changes in the three phenomena are not exactly synchronous, i.e., the point-to-point behavior differs in each. Indeed, there is somewhat different behavior in detail between the several VLF channels. However, the maximum intensity of every feature, including the maximum flux of electrons with $E_e \gtrsim 10$ kev (not shown in Figure 12, but see part 2), occurs at the same time (or place) to within about 2 sec (or about 16 km). These maximums did not occur at precisely the same time. But then, for example, the electron spectrum was changing so greatly that the peak flux of all electrons with energy $E_e \gtrsim 10$ kev occurred about eight samples or 2 sec before the peak (1/4-sec sample) flux of electrons with $E_e \gtrsim 40$ kev. We do not expect absolutely precise point-to-point correlation among all the measurements. It is therefore reasonable to assume that the phenomena are related in some way. We discuss these relations below.

The hiss intensity did not show a strong decrease at the time of maximum auroral activity. This observation serves to support the proposition mentioned earlier that decreases in VLF auroral hiss intensity, observed on the ground, during the presence of intense and active auroras are attributable to the attenuation of the VLF hiss radiation in the lower ionosphere.

Grouped in Table 1 are estimates of the maximum intensities of each phenomena detected by Injun 3 for the events being considered. The energy flux of the VLF radiation, having frequency components less than 10 kc/s, has been calculated from the VLF spectrum analyzer measurements. The upper frequency limit for an auroral hiss emission may be as high as 30 kc/s [*Helliwell*, 1962]. The total energy of VLF radiation may, therefore, be much larger than the VLF energy flux given in Table 1. It is assumed in these calculations that the quasi-longitudinal approximation for the index of refraction is valid and that the ambient electron density at the satellite is 5×10^5 electrons/cm^3. This electron density at 300-km altitude has been estimated on the basis of the electron density profiles measured during relatively undisturbed conditions at lower latitudes [*Ratcliffe*, 1960; *Budden*, 1961]. In the auroral events being considered, the electron density may very well be enhanced at 300 km by the precipitated particles exciting the aurora. The VLF energy flux calculation is, however, relatively insensitive to the ambient electron density, the proportionality factor being $N_e^{-1/2}$. The calculations and assumptions leading to the stated electron energy flux and auroral light flux are discussed in part 2 and part 4 of this series.

From Table 1 we note that the energy flux of electrons exceeds the energy flux of the auroral hiss by a large factor and that this factor is markedly different for the two cases considered, being 10^7 for the March 3 event, and 10^4 to 10^5 for the February 28 event. Considering the question of whether the precipitated electrons observed at Injun 'cause' the VLF radiation or vice versa, it seems clearly reasonable, in terms of efficiency, that via some suitable coupling mechanism particle energy may be converted to VLF radiant energy. Considering the other possibility, that VLF electromagnetic radiation acts to accelerate those magnetospheric electrons that are being precipitated into the atmosphere, it would indeed seem to be very remarkable that the coupling mechanism, VLF to particles, could be so efficient that, of the original VLF flux acting to accelerate the particles, only 10^{-7} of this flux could be detected at the altitude of the satellite. We conclude that these measurements strongly suggest that VLF electromagnetic radiation does not act as the primary energy source for the acceleration of the electrons observed by Injun during intense electron precipitation events.

The Injun measurements of the magnetic spectral density of VLF radiation in the ionosphere also provide experimental evidence supporting a conclusion by *Kellogg* [1963] that VLF electromagnetic fluctuations apparently cannot explain intense precipitation. It is sug-

TABLE 1. Maximum Intensity of Each Phenomenon Observed by Injun 3 in Two Auroral Hiss Events

	0720 to 0725 UT, March 3, 1963	0949 to 0954 UT, Feb. 28, 1963	Units
L of maximum intensity	8.5	8 to 12	
Local time of maximum intensity	2100	0100	
Altitude of maximum intensity	300	300	km
Energy flux: VLF radiation, less than 10 kc/s*	8.0×10^{-7}	3.0×10^{-7}	erg cm^{-2} sec^{-1}
Energy flux: precipitated electrons $E_e \geq 10$ kev	10.0	<0.1	erg cm^{-2} sec^{-1}
Energy flux: visible auroral light (estimated to be 3 times 3914 A)	0.6	0.1	erg cm^{-2} sec^{-1}
Wide-band magnetic field strength (7-kc/s noise bandwidth)†	9×10^{-3}	4×10^{-3}	rms gamma
Flux: precipitated electrons, $E_e \gtrsim 10$ kev (2-sec averages)	7×10^{7}	$<2 \times 10^{6}$	particles cm^{-2} sec^{-1} ster^{-1}
Flux: precipitated electrons, $E_e \gtrsim 40$ kev (2-sec averages)	2×10^{6}	6×10^{3}	particles cm^{-2} sec^{-1} ster^{-1}
Flux: trapped electrons, $E_e \gtrsim 40$ kev (2-sec averages)	2×10^{6}	6×10^{3}	particles cm^{-2} sec^{-1} ster^{-1}
Flux: auroral light, 3914 A	$40\begin{Bmatrix}+80\\-30\end{Bmatrix}$	$8\begin{Bmatrix}+16\\-4\end{Bmatrix}$	kilorayleighs

* See text for details of this calculation.
† See Figure 3 for frequency response of wide-band signal strength measurements.

gested, therefore, that the precipitated electrons caused both the visible aurora and the VLF hiss emission.

We shall now assume that the variations in the phenomena observed in the March 3 event were small in the time it took for the satellite to pass over them, i.e., over times of about three minutes. The observations were at local time around 9 PM, and it is reasonable to assume that they were made during the relatively quiescent development phase of the aurora several hours before the breakup active phase.

If it is assumed that the phenomena observed in the March 3 event were time stationary for times of the order of 3 minutes, the VLF measurements in Figure 12 are interpreted as giving the spatial extent of the ionosphere illuminated by the VLF hiss radiation. We shall now compare the geomagnetic L shell boundaries of the hiss radiation with the L shell boundaries of the stream of precipitated particles. This comparison will be made from measurements at the satellite altitude of approximately 300 km. For a given phenomenon we shall define the position of the L shell boundary, at a constant altitude, to be those points where the intensity measurements associated with the phenomenon are one-tenth of the peak intensity occurring. These bounds can be considered to define a region, at the satellite altitude, upon which the major fraction of the energy associated with a phenomenon is incident.

The L shell boundaries of the precipitated particle stream in the March 3 event were roughly estimated using the response of detector 5 and the intensity of the auroral optical emission. The estimated bounds (one order of magnitude below the peak intensity) of the precipitated particle flux is shown as $\delta\Lambda_P$ in Figure 12. The estimated bounds of the VLF hiss radiation are shown as $\delta\Lambda_H$ in Figure 12. An order of magnitude change in the magnetic spectral density has been taken to be a factor of $(10)^{1/2}$ in the wide-band VLF signal strength. Expressed in terms of invariant latitude Λ [$L \cos^2 \Lambda = 1$], the spatial extent of the hiss illuminating the lower ionosphere, determined using the above bounds, was approximately $\delta\Lambda_H = 9.5°$. The spatial extent of the particles being precipitated into the atmosphere, as determined from detector 5 and the auroral optical emission, using the previously defined boundary criterion, was approximately $\delta\Lambda_P = 3.3°$.

It appears, from these considerations, that

the region of the ionosphere illuminated by the major fraction of the VLF hiss energy is approximately three times as large, in terms of invariant latitude, as the region of the atmosphere into which the major fraction of the particles are being precipitated. If it is assumed that the VLF hiss is generated within the L shell boundaries of the precipitated particle stream, it would appear that the VLF hiss emission must occur at sufficiently high altitudes that the VLF radiation can illuminate a range of Λ values, at the satellite altitude, considerably larger than the range of Λ values over which particles are being precipitated into the atmosphere.

We now very briefly examine some features which were not included in the above discussion, but which do not alter significantly the general conclusion. It is clear that the particle detectors can obtain a representative sample of the particle flux over only about a cyclotron radius, i.e., over some tens of meters. Still assuming a phenomenon unchanging over three minutes of time, the latitude or L profile of particle precipitation is a swathe some tens of meters wide. The photometric latitude profile, on the other hand (with an optical field of view of about 10°), is a swathe some 40 km wide. Thus the two measurements of auroral light and particle precipitation are not strictly comparable, even if one does not introduce the other variables of electron energy spectrums. Now we have little knowledge of the characteristic dimensions of the VLF at the satellite altitude, but we can speculate as to what they may be. For example, a representative minimum dimension would be the wavelength. Consider 3 kc/s VLF; a wavelength is of the order of 100 km to 1 km, depending on the (unknown) refractive index (n). Thus the VLF measurements at Injun 3 are representative of the VLF radiation over at least several kilometers, and perhaps over several hundred kilometers.

Now reverting to Figure 12, it can be seen that the low-latitude 'edge' of the intense VLF (as defined above and marked in Figure 12) is some 2° below the onset of the auroral and the particle intense fluxes, while the high-latitude 'edge' of the VLF is some 4° above the cessation of the other intense fluxes. When we consider the arbitrary definition of the 'edge,' the discrete nature of the sampling, and the differing characteristic lengths of the three phenomena, it appears reasonable to suggest that the auroral and particle edges were roughly equidistant in latitude or geographic distance from the corresponding edges of the VLF. The VLF then appears to become intense and cease to be intense some 3° of latitude (or some 300 km) before and after the respective locations of the intense auroral and particle fluxes. This distance can be taken as a measure of the characteristic width of the VLF radiation at the satellite altitude. This width is at least a few wavelengths. It may be this large because the VLF source was far from the satellite, i.e., at a high altitude.

If we measure the difference between the onsets and cessations of the several phenomena in units of L, the low-latitude difference is only 1 earth radius, but the high-latitude difference is about 7 earth radii. The simple concept of L as an equatorial radial distance cannot hold here, however, because it seems likely that the high-latitude edge of the particle flux delineates the magnetic field line passing through a boundary of the magnetosphere (see part 4).

Analysis of the Observation of February 28, 1963

The data shown in Figure 13 are a further example of coordinated observations of VLF, particle fluxes, and auroral light, selection of an 'event' being solely on the basis of high intensity of auroral light without reference in the first place to either VLF or particle fluxes. It is apparent from Figure 13 that this unbiased method of selection has resulted in our choosing a pass in which any generalizations (such as those drawn from Figure 12) are not possible.

The auroral optical emissions in this event are more complex than those of Figure 12. Again we assume for discussion that the phenomena were stationary in time. Then the aurora showed a slowly varying component extending from $L \sim 6$ to $L \sim 14$, with a maximum at $L \sim 7.5$. In addition, three well-defined emission peaks occurred, one at $L \sim 9.5$ and the other two at $L = 12$. Synchronous variations occurred in the emissions at both 5577 A (from oxygen) and 3914 A (from nitrogen), as discussed in part 4.

The VLF spectrum analyzer indicates that the VLF radiation detected at the satellite is

a noise spectrum extending over a wide range of frequencies. The magnetic spectral density shows marked variations from channel to channel. These variations change with time and indicate that the frequency spectrum of the VLF hiss radiation at the satellite is changing with the motion of the satellite through space and time. The spectral density tends to increase at higher frequencies. We identify the VLF emission as an auroral hiss emission on the basis of the characteristic wide-band noise spectrum and the association with the auroral optical emissions. From the wide-band signal strength measurement, it appears that the VLF hiss is closely associated with the sharp auroral emission peaks but is not closely related to the slowly varying auroral emission extending from $L = 6$ to $L = 14$.

The intensity of precipitated electrons with $E_e \gtrsim 40$ kev shows very little apparent relation to either the VLF or the aurora. The particle fluxes and the auroral light show variations in the same sense, but there is no consistent quantitative relation between them in this event. This is a relatively low-intensity event, and the insensitive detectors of low-energy ($E_e \sim 10$ kev) electrons showed little response (see discussion in part 4 about the relative roles of electrons of different energies in exciting auroras).

Now the VLF intensity in Figure 13 changes more rapidly and by greater amounts than it does in Figure 12. In fact, all the phenomena are so variable that it is possible that an active or breakup phase of an aurora is being observed. The local time of the observation, about 1 AM, encourages such a view.

One method of distinguishing spatial from temporal variations is as follows. If the field of view of the photometers at the usual auroral altitude of ~100 km is X, and if the photometers see significant variations in a time T such that $T \ll X/V$, where $V =$ the velocity of the satellite, then the variation in light intensity is (at least partially) a temporal effect. If $T \gg X/V$, it may be temporal or spatial. In Figure 13, for the photometers $X = 40$ km, and, considering the two close maximums at $L \sim 12$, $V = 8$ km/sec, and $T \sim 8$ sec. Therefore the photometers cannot be used to resolve whether these are spatial or temporal variations.

If we accept 300 km as a representative characteristic dimension for VLF by using the somewhat weak arguments in the preceding section, from Figure 13 it is apparent that $T \ll X_{VLF}/V$ for several peaks. Again this leads to a conclusion that temporal variations are considerable in the pass of Figure 13 and that the different characteristic dimensions of the three detectors of the three phenomena lead to imperfect correspondence one with the other.

We might consider the two highest peaks of light in Figure 13 as coming from auroral arcs. *Morozumi* [1962] has found that VLF hiss was not characteristic of all auroras but had a close association with auroral arcs. However, this is merely speculation here, and it cannot be resolved for this example because clouds obscured the ground-based observations.

Discussion and Summary

Throughout this study, it has been assumed that the presence of the satellite in the medium does not modify significantly the VLF phenomena studied. It is also assumed that the presence of the large satellite shell near the loop antenna does not modify significantly the amplitude measurements. Though both assumptions appear reasonable, neither is proven here to be valid.

VLF measurements in the ionosphere with Injun 3 have been characterized by remarkably large VLF magnetic intensities relative to ground-based measurements. In about 15 hours on the ground, only three whistlers and no VLF emissions were detected with the satellite VLF receiver and antenna. The same VLF receiver and antenna in orbit has detected many long-hop whistlers and has detected magnetospheric VLF emissions for 24 per cent of the total observation time during January 1963. On one occasion, a wide-band VLF hiss emission was observed in the ionosphere for which the magnetic spectral density of the hiss radiation was 3.6×10^{-7} (gamma)^2 (c/s)$^{-1}$. This magnetic spectral density was a factor of 10^6 greater than the maximum observed on the ground in previous studies of a similar phenomena by Ellis. A notable exception to the generally large VLF intensities observed at the satellite is the background noise level of sferic impulses (short fractional-hop whistlers). The sferic background noise level is much lower in the upper ionosphere than on the ground. These observations may be attributed, in part, to the ionospheric

attenuation of electromagnetic waves at VLF frequencies. It seems probable, in the case of VLF magnetospheric emissions, that additional factors may be operating which increase the intensity of the magnetic component of the VLF radiation relative to ground-based observations. It has been suggested, for instance, that ducting of VLF radiation may occur in the magnetosphere. A very intense VLF power flux may be observed when the satellite is in a propagation duct or is close to the source of the VLF emission.

Hiss having frequencies less than 1 kc/s and chorus are the most common VLF electromagnetic emissions observed at the satellite. ELF hiss having frequency components as low as 200 cps is commonly observed at the satellite and is often characterized by a sharply defined upper frequency limit. The frequency response characteristics of the VLF receiver have made absolute measurements in this frequency range difficult.

Direct measurements of the amplitude of the VLF radiation from chorus emissions have been made in the ionosphere with Injun 3. These measurements have been analyzed for satellite local time coordinates between 0800 and 1300. The measurements analyzed extended over a three-day period. The amplitude of the chorus radiation at the satellite was found to have a systematic variation with the geomagnetic L parameter. This variation was highly reproducible from pass to pass. The amplitude of the VLF chorus radiation illuminating the ionosphere shows a well-defined peak at $L = 5$ for the three-day period studied, which was geomagnetically disturbed (average K_p of 5). The amplitude of the magnetic component of the VLF chorus radiation at $L = 5$ was typically 8×10^{-3} gamma in the frequency band 0.5 to 7.0 kc/s.

When the frequency-time spectrums of the chorus radiation were compared at the same L value for different passes, the character of the spectrums was found to vary markedly in times less than one orbit period (about 2 hours). Chorus emissions have been observed for which the discrete emissions occur over a narrow band of frequencies. In some instances, the center frequency of banded chorus emissions is found to be remarkably independent of L. This observation suggests that the VLF radiation from the same chorus source region was being viewed by the satellite VLF antenna over a wide range of L value.

When all the instrumentation on the satellite was used to analyze optical and VLF emissions and particle fluxes in auroras, the rigor of the conclusions was greatly weakened by our inability to resolve with certainty phenomena varying in space from those varying in time. More extensive coordinated studies with ground-based observatories are under way to resolve these problems. Nevertheless, in these preliminary studies, several conclusions can be made.

First, in the March 3 pass, when reasonably stable phenomena were measured, there appeared to be a close relationship between auroral optical emissions, particle precipitation, and VLF emissions. Such deviations from a perfect interrelationship as did exist may be thought of as arising from such factors as the different characteristic dimensions sampled by the different detectors, and the variable electron spectrums. On this basis, the characteristic dimension of the VLF emission at ~300-km altitude was some 300 km. It then appears consistent with the data to assume that the VLF emissions were generated in much the same region of space as were the precipitated electrons, or at least that both were generated on the same magnetic shell, perhaps at similar altitudes but perhaps not. Furthermore, this magnetic shell is near the outer edge or boundary of the ordered geomagnetic field lines passing through the magnetosphere, outside of which no durable trapping of particles is possible.

The relative magnitudes of the several phenomena, as listed in Table 1, justify the assumption that the aurora, of international brightness coefficient II, was caused by precipitated electrons, and that detector 5 measured the high-energy part of this electron flux. We have not conclusively shown whether the precipitated particles and others (see part 3) 'caused' the VLF radiation or whether the opposite situation prevailed and VLF radiation acted to accelerate the precipitated particles, or whether indeed something else (which we did not measure) caused them both. Comparison of the energy flux of precipitated electrons and the energy flux of the VLF radiation gives support to the contention that, via some suitable coupling mechanism, some energy of the precipi-

tated corpuscular radiation is converted to VLF electromagnetic energy.

The data from the pass of February 28 serve mainly to illustrate that generalizations from the pass of March 3 may be subject to doubt. The interpretations of both passes can be reconciled if we assume that the measurements of February 28 were rendered confusing by significant temporal changes in times of the order of tens of seconds, and this assumption appears reasonable. Even in this variable aurora, however, our earlier suggestion, that the VLF hiss is generated near the high-latitude (or large L) termination of trapping, appears consistent with the observations.

Only a small fraction of the available data have been analyzed here in this preliminary report. Further studies are being made of the interrelationship of VLF and auroras in which ground-based observations will also be used. It is to be expected that further experimental studies will elucidate many points, but further theoretical study is also essential. In particular, we must seek to determine the causal relations, if any, between particle fluxes and VLF. Treatments such as that by *Dowden* [1963] would imply that particle fluxes cause VLF. Treatments such as that by *Kellogg* [1963] would imply that VLF causes acceleration of particles, hence precipitation and auroras. It may be that both are valid on some occasions. Study of the March 3 event suggests that the energy balance is as follows (see Table 1):

VLF energy flux less than 10 kc/s	$= 8.0 \times 10^{-7}$ erg cm^{-2} sec^{-1}
Electron energy flux	$= 10$ ergs cm^{-2} sec^{-1}
Auroral light energy	$= 0.6$ erg cm^{-2} sec^{-1}

These data are subject to considerable experimental uncertainties, and, in particular, we do not know the electron density in the neighborhood of the satellite, nor do we know to what extent the presence of the satellite shell perturbs the measurements of the absolute amplitude of the VLF radiation.

Appendix

General. An extended treatment of the VLF experiment and its calibration is given by Gurnett and Frohwein (to be published). A brief treatment is given here to clarify some of the interpretations of the results presented earlier.

The wavelength of the VLF radiation studied by Injun 3 is much larger than the loop antenna diameter. The antenna is so oriented by the satellite orientation magnet (see part 1) that the geomagnetic field vector $\mathbf{B}_0$ is parallel to the plane of the loop. The electronic stimulus for the VLF electronics is the very small emf induced in the antenna by the VLF electromagnetic field. The emf can be interpreted as arising from the circularly polarized H component whose plane of rotation is perpendicular to the direction of $\mathbf{B}$ [*Brandstatter*, 1963]. The magnitude of the emf (v) is given by the following treatment.

Let $\mathbf{n}$ be a unit vector perpendicular to the plane of the loop having N turns and area A. (With Injun 3, $N = 50$ and $A = 0.073$ m^2.) Then

$$v = NAd/dt(\mathbf{B}\cdot\mathbf{n})$$

where $\mathbf{B} = \mu_0 \mathbf{H}$, or, if $\mathbf{B}\cdot\mathbf{n} = B_p \exp(j\omega t)$,

$$v = j\omega NAB_p \exp(j\omega t) \qquad (1)$$

Thus, the amplitude of the emf for a constant rms amplitude of $\mathbf{B}\cdot\mathbf{n}$ is proportional to the angular wave frequency ω. It was considered desirable to have a system in which the frequency response was almost uniform, and so the preamplifier includes a network having a frequency response proportional to $(\omega)^{-1}$.

The preamplifier signal, limited to a frequency band of approximately 0.5–7.0 kc/s, is normalized to a constant amplitude by an automatic gain control (AGC) circuit. This normalized signal is used to phase modulate (PM) the 1.5-watt telemetry transmission at 136.860 Mc/s. Normalization of the modulation signal amplitude is necessary to efficiently modulate the telemetry transmission. When the satellite transmission at 136.860 Mc/s is demodulated with a receiver, the receiver analog output signal has a frequency spectrum faithfully reproducing the spectral character of $\mathbf{B}\cdot\mathbf{n}$ in the 0.5- to 7.0-kc/s frequency range. The relative frequency response of the wide-band VLF system including the antenna, preamplifier, AGC circuit, PM transmitter and receiver, is shown in Figure 3. This measurement was made by holding the gain of the AGC circuit constant. Since the frequency response of the transmitter and receiver system are very nearly independent of frequency (in the range considered), Figure 3 gives essentially the frequency response of the AGC circuit for constant gain. Absolute amplitude information

is destroyed by the AGC circuit in the VLF analog transmission. The AGC feedback voltage, however, provides a measure of the wide-band absolute signal strength from the preamplifier. The frequency response of the AGC circuit provides the proper weighting function for this measurement at different frequencies. The AGC circuit time constant is approximately 0.2 sec. The wide-band signal strength measurement (AGC feedback voltage) is sampled instantaneously at 4-sec intervals by an analog to digital converter. The output from the wide-band signal strength measurement is, therefore, representative of the magnetic spectral density integrated over the receiver bandwidth using the frequency response curve, shown in Figure 3, as a weighting function.

The VLF spectrum analyzer provides measurements of the magnetic spectral density of the VLF electromagnetic wave coupling the loop antenna at six frequencies. In the spectrum analyzer, the frequency spectrum from the preamplifier is translated upward in frequency by 100 kc/s. The spectrum analyzer channels are defined with magnetostrictive filters. The 3-db bandwidth of each filter is approximately 50 cps. The amplitude of the signal in each channel is measured by an envelope detector. The dynamic range over which the detector is linear is approximately 40 db. To provide an extended dynamic range, an attenuator was included between the preamplifier and the spectrum analyzer. The dynamic range may be shifted in two 20-db steps by remote commands from the ground. The amplitude measurement from the envelope detector was processed by an analog to digital converter which generated a number proportional to the logarithm of the minimum amplitude occurring in the time interval since the previous sample was transmitted. The analog to digital converter has sixteen quantizing steps. The 40-db dynamic range of the spectrum analyzer is, therefore, quantized into sixteen steps, approximately 2.5 db per step. The measurement of the minimum amplitude over a period of time was used in order that the spectrum analyzer measurement would give the amplitude of the slowly varying noise spectrum ($\tau \gtrsim 2$ sec) and would ignore transient noise impulses ($\tau \lesssim 0.1$ sec), like lightning. The sampling rate most commonly used in orbit is 1 sample every 2 sec.

Calibration before launch. To calibrate the VLF experiment, we must choose parameters descriptive of the VLF magnetic component ($\mathbf{B}\cdot\mathbf{n}$) detected with the antenna. Because the spectral nature of many VLF emissions (especially hiss) closely resembles a banded noise spectrum, it was decided that random noise would be used to calibrate the absolute amplitude measurements. Random noise signals are usually described by a spectral density $G(f)$. $G(f)\Delta f$ is the average power or mean square signal in the frequency interval Δf. We shall use $B(f)$ to denote a magnetic spectral density. We shall define the rms signal strength B_r by the relation

$$B_r^2 = \int B(f)\, df \tag{2}$$

The spectral power density of an electromagnetic wave in a nonconducting medium having index of refraction n is given in terms of $B(f)$ and B_r as

$$\mathbf{S} = \mathbf{E} \times \mathbf{H}$$

$$S = \frac{1}{n}\sqrt{\frac{\mu_0}{\epsilon_0}}\left(\frac{B_r}{\mu_0}\right)^2 \text{ watts (m)}^{-2} \tag{3}$$

$$S(f) = \frac{1}{n}\sqrt{\frac{\mu_0}{\epsilon_0}}\frac{B(f)}{\mu_0^2} \text{ watts (m)}^{-2}\text{(c/s)}^{-1} \tag{4}$$

The units used for $B(f)$ will be (gamma)^2 (c/s)$^{-1}$ (1 gamma = 10^{-9} weber (m)$^{-2}$). The units used for B_r will be rms gamma.

It was decided that the spectrum analyzer channels and the wide-band signal strength measurement would, in principle, be calibrated by applying a constant spectral density, magnetic noise signal, $B_0(f)$ normal to the plane of the loop antenna. The spectrum analyzer calibration is therefore the dependence of the digital readout, from each spectrum analyzer channel, on the applied magnetic spectral density $B_0(f)$. For the wide-band signal strength, a slightly different interpretation of the applied stimulus is used. For a given constant magnetic spectral density $B_0(f)$ applied to the antenna, we shall assign to the wide-band signal strength digital readout a quantity given by $B_w = [B_0(f)\,\Delta f]^{1/2}$, $\Delta f = 7$ kc/s. B_w will be called the wide-band magnetic field strength. The noise bandwidth Δf of a circuit is defined as the bandwidth of an ideal rectangular passband, having the same maximum gain and passing the same average power, from a white-noise source, as the circuit under consideration

[*Hancock*, 1961]. The noise bandwidth Δf for the AGC circuit was determined, by graphical integration of the frequency response of the AGC circuit (Figure 3), to be approximately 7 kc/s. The wide-band magnetic field strength B_w will be interpreted as the square root of the integral given in (2), integrated from 0 to 7 kc/s. $B(f)$ is the spectral density of the $\mathbf{B}\cdot\mathbf{N}$ component at the loop antenna. The error implicit in this interpretation is given by the frequency response of the AGC circuit shown in Figure 3. Above 1 kc/s the maximum error in this interpretation is about 4 db. Below 1 kc/s the error in this interpretation becomes progressively larger.

A direct calibration of the VLF experiment at maximum sensitivity by applying a magnetic field to the antenna is impossible because of the continually present sferic and power system noise. The Injun 3 VLF experiment was calibrated by using an electrical analog of the VLF antenna. The network was designed such that the electrical input voltage signal was directly analogous with the $\mathbf{B}\cdot\mathbf{N}$ component. The electrical analog of the antenna is shown in Figure 14. The 1.6-mh inductance and the 0.8-Ω resistance correspond to the inductance and resistance of the loop antenna. (Distributed capacitance effects were negligible.) The response of the RC network to a signal of angular frequency ω is given by $v = j\omega RCV_1$, when $RC\omega \ll 1$. If we compare this expression with (1) we can establish the following analogy

$$B_r = (RC/NA)\,V_1 \qquad RC\omega \ll 1 \qquad (5)$$

or, in terms of spectral densities,

$$B(f) = (RC/NA)^2 G_1(f) \qquad RC\omega \ll 1 \qquad (6)$$

The relationship in (6) follows from (5) as a result of linear network theory [*Hancock*, 1961]. The voltage spectral density $G_1(f)$ shown in the diagram of the VLF calibration (Figure 14) can therefore be interpreted as a magnetic spectral density applied to the antenna had the antenna been connected to the VLF instrument. The values for C and R were measured on an audio-frequency bridge and were found to be $C = 0.101$ $\mu f \pm 1$ per cent and $R = 0.203$ ohm $\pm$ 1 per cent, clearly $RC\omega \ll 1$. The quantities N and A are also known, and so $B(f)$ can be calculated if $G_1(f)$ is measured.

The spectral density of the white noise source, used in the VLF calibration, was measured at various frequencies with a Donner wave analyzer and was found to be constant to within $\pm$1.0 db over the frequency range considered. The spectral density $G_0(f)$ was measured, during the calibrations, by measuring the true rms voltage at the output of a low-pass filter (LPF) having a sharp cutoff at 7 kc/s. A variable attenuator was used to control the amplitude of $G_1(f)$. The output of the VLF experiment consisted of a sequence of numbers from the six spectrum analyzer channels and from the wide-band signal strength measurement. Since the signal being measured is random noise, the digital outputs from the VLF experiment have random fluctuations. Using a random noise input signal, we found the standard deviation of the spectrum analyzer digital readout to be approximately $\sigma = 0.37$ unit. The digital measurements from the spectrum analyzer were averaged for approximately twenty successive samples during the calibration of the instrument. A typical calibration of a spectrum analyzer channel at 25°C is shown in Figure 15. The receiver noise level can be estimated, at each of the six frequencies, from the break in the curves at low signal levels. The receiver noise level is approximately 5.0×10^{-11} (gamma)^2 (c/s)$^{-1}$.

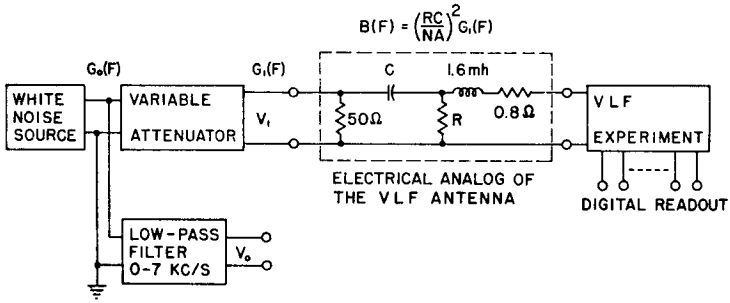

Fig. 14. VLF experiment calibration.

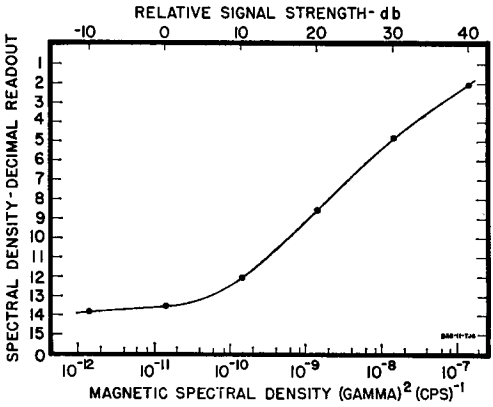

Fig. 15. Typical spectrum analyzer calibration (2.7-kc/s channel).

Using this noise level and (4) with $n = 1$, the receiver noise level, in terms of the VLF power spectral density detectable on the ground, is approximately 1.5×10^{-14} watt $(m)^{-2}$ $(c/s)^{-1}$. In general, the receiver noise level increases at lower frequencies, especially the 700-cps channel. The variations in the analyzer gain and receiver noise level with temperature are shown in Table 2. The numbers shown in the table are the decimal readouts for the various frequency channels averaged for approximately 20 successive samples. The results of the calibration of the wide-band magnetic signal strength measurement have been shown in Figure 16. The variations in these measurements with temperatures from 10°C to 25°C were of the order of the quantizing errors associated with the measurement.

The performance of the VLF experiment in orbit. It is desirable to check the calibration of the VLF experiment periodically in flight. No system was included in the Injun 3 VLF experiment for postlaunch calibrations. A good check can be made on the absolute gain of the instrument by comparing the receiver noise levels in flight with those noted in the preflight calibrations. Receiver noise levels, in terms of the digital readouts from the spectrum analyzer channels, are shown for several postlaunch dates in Table 2. These measurements are the average of 20 successive readouts for conditions when no VLF radiation was thought to be detectable. The 700-cps channel has shown a consistently higher noise level in flight than in the prelaunch calibrations. It is not known whether these measurements are indicative of VLF radiation being detected at this frequency or whether the gain of this channel has in fact shifted. The 700-cps channel has shown good correlation with the wide-band signal strength measurements for cases where the VLF emissions were less than 1 kc/s. A large percentage of the time the 700-cps channel is saturated, possibly indicating strong VLF signals at this frequency. The validity of the calibration of the 700-cps channel cannot be established at this time. The remaining spectrum analyzer channels show postlaunch noise levels in good agreement from month to month, and possibly slightly higher (less than 2.5 db) than the prelaunch calibrations. Receiver noise level measurement obtained with the wide-band VLF signal strength measurement has in every case read 3, in agreement with the prelaunch calibrations (Figure 16). Checks of the

TABLE 2. VLF Spectrum Analyzer Gain and Noise Level Variations

Center Frequency, cps	Prelaunch: Absolute Gain vs. Temperature; Signal Input, 1.2×10^{-8} $(gamma)^2$ $(c/s)^{-1}$			Prelaunch: Receiver Noise Level vs. Temperature			Postlaunch: Receiver Noise Level Date					
	−5°C	10°C	25°C	−5°C	10°C	25°C	12/26/62	1/8/63	2/8/63	3/11/63	4/5/63	5/1/63
700	5.5	4.25	4.5	10.5	8.5	9.50	4.1	3.9	4.35	3.85	4.35	4.15
2700	4.75	4.50	4.75	13.25	13.50	13.75	12.35	12.55	12.50	12.00	12.50	12.15
4300	3.25	3.25	3.50	12.75	13.25	14.00	13.05	13.05	12.65	12.95	12.75	12.35
5500	4.25	4.00	4.25	13.00	13.75	14.00	13.50	13.55	13.35	12.85	13.40	13.00
7000	4.00	4.00	4.50	13.50	14.00	14.50	14.15	14.05	14.00	13.45	13.80	13.25
8800	4.00	4.00	4.25	13.50	14.00	14.50	14.10	14.15	13.80	13.85	14.10	13.90

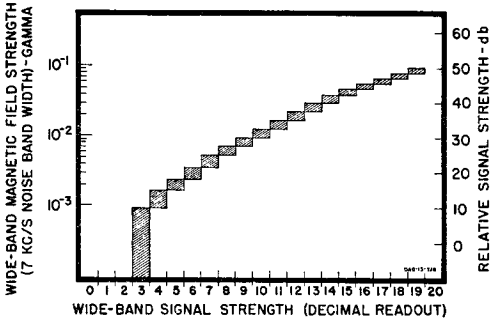

Fig. 16. Wide-band signal strength calibration.

AGC calibration relative to the spectrum analyzer calibration, by piecewise integration of the magnetic spectral density of wide-band hiss events, have shown, in general, agreement to within ± 2.5 db. In view of the uncertainty associated with the perturbation caused by the satellite shell on the absolute measurement of the VLF field, the instrumental calibration errors have not been stated in the results presented.

Possibility of false VLF signals in orbit. VLF data from Injun 3 could be subject to contamination in several ways. For example, the satellite is moving through the ionized medium, and we might suggest that it either modifies naturally occurring VLF processes in some way or perhaps that it 'triggers,' or initiates, VLF emissions that would not have occurred in its absence. We argue against the first possibility by showing that the spectral character of VLF emissions observed at the satellite is like those commonly observed with ground-based VLF receivers (compare Figure 6 of this note with those shown by *Gallet* [1959]). We regard the second possibility as unlikely (we certainly cannot claim that it *never* occurs) because we observe VLF signals sporadically over a wide range of altitudes, from as low as 250 km to as high as 2800 km, and the ionospheric properties change so greatly over this range that we cannot visualize any threshold of triggering VLF which would be constant over this range.

One of the major problems in any VLF study is contamination by electronically generated noise nearby. With Injun 3, this is essentially what we call 'payload noise.' We took many actions to minimize payload noise, and these are discussed in a technical study (Gurnett and Frohwein, to be published). In ground tests, each detector was activated, and we checked to see that its response (i.e., to particle radiation or light, etc.) did not in any way interact with the VLF measurements.

Before April 5, 1963, no evidence had been found from the data obtained from the satellite in flight which suggested that any form of radiation originating from the satellite was detectable with the VLF experiment. Starting April 5, 1963, a periodic clicking with a variable period, usually about two seconds, has been occasionally heard from the wide-band signal telemetered to the ground. This signal is presumed to originate from within the satellite electronics system. It has been established that this interference source, which is of a transient nature, is not of sufficient amplitude to be measurable with either the wide-band signal strength or the spectrum analyzer measurements. All data presented in this analysis were obtained before April 5, 1963.

No VLF signal radiated from a man-made source has ever been identified from observations in the ionosphere with the Injun 3 VLF experiment.

Acknowledgments. We are very grateful to Dr. Jerome Fregeau for his sympathetic assistance. Telemetry reception was obtained for this study by Roger Tetrick of Goddard Space Flight Center and D. R. Hansen of the Prince Albert Radar Establishment. Many people assisted in design and construction of Injun 3, and we particularly thank C. Laughlin, G. Frohwein, C. Kime, M. Risk, and S. Clark (for payload and VLF), L. Frank, J. Craven, and H. Taylor (for other detectors), all at SUI. Other assistance was provided by T. Baker, R. Bradley, and G. Jamieson, of Raytheon Co.; G. Huddleston, P. Coleman, and D. Gleason, of the AeroGeoAstro Co.; and J. Jekerly and L. Miner of Collins Radio Co. The program would not have been possible without the help of Dr. J. A. Van Allen, who also gave much valuable advice in discussion of the results. M. Votaw of the Naval Research Laboratory was very helpful throughout the whole enterprise. Many valuable suggestions during design of the VLF experiment came from Dr. R. Gallet and Messrs. R. L. Hanes and J. M. Watts of the National Bureau of Standards. Dr. A. J. Dessler was of great assistance in discussion of these results.

We are very grateful to Mr. G. Frohwein of SUI and to Dr. F. S. Atchison of the Naval Ordnance Laboratory for preparation of spectrograms.

This research was supported in part by the Office of Naval Research under contract N9onr-93803 and by the National Aeronautics and Space Administration under grant NsG-233-62.

References

Allcock, G. McK., A study of the audio-frequency phenomena known as 'dawn chorus,' *Australian J. Phys., 10,* 286, 1957.

Barrington, R. E., and J. S. Belrose, Preliminary results from the VLF receiver aboard Canada's Alouette satellite, *Goddard Space Flight Center Publ. X-615-63-36,* 1963.

Brandstatter, Julius J., *An Introduction to Waves, Rays, and Radiation in Plasma Media,* p. 77, McGraw-Hill Book Company, New York, 1963.

Budden, K. J., *Radio Waves in the Ionosphere,* p. 9, Cambridge University Press, London, 1961.

Cain, J. C., I. R. Shapiro, J. D. Stolarik, and J. P. Heppner, A note on whistlers observed above the ionosphere, *J. Geophys. Res., 66,* 2677–2680, 1961.

Carpenter, D. L., Electron-density variations in the magnetosphere deduced from whistler data, *J. Geophys. Res., 67,* 3345, 1962.

Dowden, R. L., Doppler shifted cyclotron generation of exospheric very-low frequency noise ('hiss'), *Planetary Space Sci., 11,* 361, 1963.

Ellis, G. R. A., Low frequency electromagnetic radiation associated with magnetic disturbances, *Planetary Space Sci., 1,* 253, 1959.

Gallet, R. M., The very-low-frequency emissions generated in the earth's exosphere, *Proc. IRE, 47,* 211, 1959.

Gallet, R. M., and R. A. Helliwell, Origin of 'very-low-frequency emissions,' *J. Res. NBS, 63D*(1), July-August 1959.

Hancock, J. C., *The Principles of Communication Theory,* p. 150, McGraw-Hill Book Company, New York, 1961.

Helliwell, R. A., *Stanford Electronics Lab. Publ. 62-024,* 1962.

Helliwell, R. A., and M. G. Morgan, Atmospheric whistlers, *Proc. IRE, 47,* 200, 1959.

Hines, C. O., Heavy-ion effects in audio-frequency radio propagation, *J. Atmospheric Terrest. Phys., 11,* 36, 1957.

Jones, D. L., R. M. Gallet, J. M. Watts, and D. N. Frazer, An atlas of whistlers and VLF emissions, a survey of VLF spectra from Boulder, Colorado, *NBS Tech. Note 166,* January 1963.

Kellogg, P., Auroral X rays, electron bombardment, and trapped radiation, *Planetary Space Sci., 10,* 165, 1963.

Laughlin, C. D., T. Fritz, and D. Stilwell, High-latitude geophysical studies with satellite Injun 3, part 2, Intensities and spectrums of trapped electrons, *J. Geophys. Res.,* to be published, 1964.

Leiphart, J. P., Penetration of the ionosphere by very-low-frequency radio signals—interim results of the Lofti 1 experiment, *Proc. IRE, 50,* 6, 1962.

Martin, L. H., Whistlers in the Antarctic, *Nature, 181,* 1796, 1958.

Martin, L. H., R. A. Helliwell, and K. R. Marks, Association between aurorae and VLF hiss observed at Byrd Station Antarctic, *Stanford Electronics Lab. Tech. Rept. 1,* 1960.

McIlwain, C. E., Coordinates for mapping the distribution of magnetically trapped particles, *J. Geophys. Res., 66,* 3681–3691, 1961.

Morozumi, H. M., A study of the Aurora Australis in connection with an association between VLF hiss and auroral arcs and bands observed at the south geographic pole, M.S. thesis, State University of Iowa, 62-14, 1962.

O'Brien, B. J., High-latitude geophysical studies with satellite Injun 3, part 3, Precipitation of electrons into the atmosphere, *J. Geophys. Res., 69*(1), January 1, 1964.

O'Brien, B. J., C. D. Laughlin, and D. A. Gurnett, High-latitude geophysical studies with satellite Injun 3, part 1, Description of the satellite, *J. Geophys. Res., 69*(1), January 1, 1964 (also see *State Univ. Iowa Res. Rept. SUI 62-24,* 1962).

O'Brien, B. J., and H. Taylor, High-latitude geophysical studies with satellite Injun 3, part 4, Auroras and their excitation, *J. Geophys. Res., 69*(1), January 1, 1964.

Ratcliffe, J. A., *The Magneto-Ionic Theory and Its Applications to the Ionosphere,* p. 13, Cambridge University Press, London, 1959.

Ratcliffe, J. A., *Physics of the Upper Atmosphere,* p. 104, Academic Press, New York, 1960.

Smith, R. L., Propagation characteristic of whistlers trapped in field-aligned columns of enhanced ionization, *J. Geophys. Res., 66,* 3699, 1961.

Smith, R. L., and R. A. Helliwell, Electron densities to 5 earth radii deduced from nose whistlers, *J. Geophys. Res., 65,* 2583, 1960.

Smith, R. L., R. A. Helliwell, and I. W. Yabroff, A theory of trapping whistlers in field-aligned columns of enhanced ionization, *J. Geophys. Res., 65,* 815, 1960.

Storey, L. R. O., An investigation of whistling atmospherics, *Phil. Trans. Roy. Soc. London, A, 246,* 113, 1953.

(Manuscript received October 4, 1963.)